Mansoura Engineering Journal

Volume 31 | Issue 2 Article 7

12-14-2020

Theoretical and Experimental Investigation on the Absorption Refrigeration Systems.

A. Elzahaby
Mechanical Power Engineering., Faculty of Engineering., Tanta University., Tanta., Egypt

Ahmed Mohamed Kandel
Mechanical Power Engineering Department., Faculty of Engineering., El-Mansoura University., Mansoura., Egypt

A. Kabeel
Mechanical Power Engineering., Tanta University., Tanta., Egypt, kabeel6@yahoo.com

M. ElSeady
Egyptian Natural Company

Theoretical and Experimental Investigation on the Absorption Refrigeration Systems

دراسة نظرية ومعملية لدوائر التبريد بالامتصاص

A. M. Elzahaby*, A. M. Hamed**, A. E. Kabeel*, M. K. Elseady***

* Mechanical Power Engineering Department, Faculty of Engineering, Tanta University, EGYPT
** Mechanical Power Engineering Department, Faculty of Engineering, Mansoura University, EGYPT, e-mail: amhamed@mans.edu.eg
*** (Egyptian natural gas company), e-mail: mkl_mohamed@yahoo.com

ملخص البحث

في هذا البحث تم عمل نموذج رياضي لدراسة دورة التبريد بالامتصاص ذات المرحلة الواحدة. تم عمل الدراسة لنظام يعمل باستخدام محلول بروميد الليثيوم والماء أو محلول كلوريد الليثيوم والماء حيث تم دراسة تأثير تغيير درجات الحرارة عند ظروف التشغيل المختلفة على معامل الأداء للدورة ونسبة السريان (معدل ضخ المحلول المخفف إلى كمية البخار المتولدة). وأيضا تم عمل دراسة معملية لعملية توليد بخار المياه داخل المولد لدورة تبريد بالامتصاص تستخدم محلول كلوريد الليثيوم والماء. من الدراسة النظرية يتضح أن معامل الأداء يزداد مع زيادة درجة حرارة المولد وعند درجة حرارة معينة يبدأ معامل الأداء في التناقص تدريجيا كما أن معامل الأداء يزداد مع ارتفاع درجة حرارة المبخر ونقص كل من درجة حرارة المكثف والماص. ويتضح أيضا أن معدل التناقص في نسبة السريان يكون بنسبة كبيرة عند درجات حرارة مرتفعة لكل من المكثف والماص. كما تم عمل مقارنة بين البيانات التي تم الحصول عليها لكل من محلول بروميد الليثيوم والماء ومحاول كلوريد الليثيوم والماء حيث وجد أن معامل الأداء أعلى لدورة محلول كلوريد الليثيوم والماء عن دورة محلول بروميد الليثيوم والماء ونسبة السريان أقل لدورة محلول كلوريد الليثيوم والماء عن دورة محلول بروميد الليثيوم والماء. وقد تم رسم النتائج المعملية لتوضيح تأثير درجة حرارة المولد على معامل الأداء ونسبة السريان والمتغيرات الاخرى الناتجة من الدراسة العملية. أيضا تم مناقشة تأثير درجة حرارة المحلول عند الدخول للمولد ومعدل ضخ المحلول وضغط المولد على كمية بخار المياه المتولدة. حيث تبين أنه يلزم استخدام حد أدنى لدرجة حرارة المولد حتى يتم فصل بخار المياه من المحلول. من القياسات العملية تم حساب أعلى قيمة لمعامل الأداء للدورة وهى (0.812)

Abstract

In the present work, theoretical model is developed to study the single-effect absorption refrigeration cycle from the thermodynamic point of view for lithium bromide-water pair and lithium chloride-water pair. The effect of different operating temperatures on the coefficient of performance (COP) and flow ratio (FR) (the weak solution mass flow rate with reference to the refrigerant mass flow rate) are investigated. The generation process in an absorption refrigeration cycle using lithium chloride-water solution as the working pair is experimentally studied. From the theoretical study, it is found that the COP increases with an increase in generation temperature until a certain value, then it decreases slightly. The COP increases with an increase in evaporator temperature and decrease in condenser or absorber temperatures. The rate of decrease in FR is higher at higher condenser and absorber temperatures. The data obtained for lithium bromide-water pair is compared with lithium chloride-water pair It is found that the COP is higher for lithium chloride-water pair than that for lithium bromide-water pair and the FR is lower for the lithium chloride-water pair. The experimental results are plotted to illustrate the effect of generation temperature on the coefficient of performance, flow ratio and output variables. Also, the effect of the inlet solution temperature, inlet solution flow rate and generator pressure on the generated water vapor is discussed. A minimum generation temperature must be chosen to boil off the water from the lithium chloride-water solution. From the measured data a maximum coefficient of performance of 0.812 can be obtained for a single stage system.

Keywords: absorption; refrigeration; lithium chloride; lithium bromide; generation.

Accepted June 9, 2006

1- Introduction

The energy demand for air-conditioning to control temperature and humidity and for the provision of fresh air has increased continuously through the last decades especially in developed countries. This increase is caused amongst other reasons by increased thermal loads, occupant comfort demands and architectural trends. This has been responsible for the escalation of electricity demand and especially for the high peak loads due to the use of electrically driven vapour compression machines. In order to reduce the electricity consumption, the substitution of vapour compression machines by thermally driven cooling systems using renewable energy as solar energy or waste heat is a promising alternative. There are several sources of energy for production of refrigeration, the most important of which are natural gas, electricity and solar energy. This energy can be used to generate cold air or chilled water by means of a device capable of absorbing heat at low temperature from a conditioned space and rejecting it into the higher temperature of the outside air with an acceptable coefficient of performance called an absorption chiller [1].

The principle theory of absorption cycle is that a process by which cooling effect is produced through the use of two fluids (refrigerant and absorbent) and some quantity of heat input rather than electrical input as in more familiar vapor compression cycle. Absorption plants are generally classified as direct or indirect-fired and as single, double or triple effect. In direct-fired units, the heat source can be natural gas or some other fuel that is burned in the unit, indirect-fired units use steam, hot water or some other transfer fluids that bring in heat from a separate source, such as a boiler or heat recovered from an industrial process.

Closed cycle absorption systems are available today in two basic configurations, for applications above 5°C a lithium bromide-water cycle is employed and is used in refrigeration cycle. For applications below 5°C an ammonia-water cycle is employed. In comparison to the ammonia-water cycle the lithium bromide-water has a number of advantages, the principle advantages being, higher coefficient of performance COP.

In air conditioning applications of absorption refrigeration cycles, many of binary mixtures can be used as working fluids e.g., lithium bromide-water, lithium chloride-water and calcium chloride-water. Practically aqueous solution of lithium bromide is widely used as the working fluid in the absorption refrigeration cycles.

A number of authors have investigated the performance of absorption refrigeration cycles using lithium bromide-water solution [2-9] and significant progress has been achieved in this area.

A. Alaktiwi et al. [2] presented an experimental and theoretical studies on the operating characteristics of an air cooled absorption refrigeration machine operating with lithium bromide-water solution. A coefficient of performance of 0.74 is obtained.

Single effect absorption systems are limited in COP to about 0.7 and it is not suited to utilize a heat source at a temperature higher than about 100°C.

To take advantage of a higher temperature heat source, absorption systems must be configured in multistage to utilize the heat rejected from the condenser to power additional generators, thereby approximately doubling or tripling the amount of refrigerant extracted out of solution with no extra heat spent. The system use gas-fired combustors or high pressure steam as the heat source.

Double-effect absorption chillers are used for air-conditioning and process cooling in regions where the cost of electricity is high relative to natural gas. Double-effect absorption chillers are also used in applications where high pressure steam such as district heating, is readily available [10].

K. Sumathy et al. [8] presented an experimental study on two stage

absorption unit using lithium bromide-water solution, the unit was driven by hot water of temperature 60 to 75°C which can be easily provided by conventional solar hot water systems.

Little work has been done in the field of which absorption refrigeration systems use lithium chloride-water solution as the working fluid in comparison with the studies on the lithium bromide-water absorption cycles. Most of the available studies were carried out theoretically using computer simulation in order to study the different variables which affect on the cycle performance.

G. S. Grover [11] presented a theoretical study for absorption heat pump systems from the thermodynamic point of view, the COP and flow ratio were given as a function of the operating temperatures at the generator, evaporator, condenser and absorber. They also compared the data obtained with published data for lithium bromide-water absorption cycles.

G. S. Grover [12] analyzed thermodynamically the possibility to operate lithium chloride absorption heat pump systems for heating process.

S. K. Chaudhari et al. [13] designed and constructed a small glass absorption heat pump using three working pairs lithium chloride-water, calcium chloride-water and water-(1-1 by weight) mixture of lithium chloride and calcium chloride. The experiments had shown that the unit can be operated with the three systems to give actual (COP) in the range 1.16-1.48 and they have presented a comparative study for the three systems.

S. K. Chaudhari et al. [14] investigated the thermodynamic properties of aqueous solutions of lithium chloride and constructed the Enthalpy-concentration charts.

S. H. Won et al. [15] presented a theoretical study from the thermodynamic point of view for double effect lithium chloride-water absorption cycle, the COP and flow ratio were given as a function of generator temperature, condenser temperature and evaporator temperature. They also compared the data obtained with published data for lithium bromide-water cycles.

The literature review on absorption refrigeration cycles shows that, a lot of work has been done to study the lithium bromide-water refrigeration cycles theoretically and experimentally, but there is a lack of published comprehensive experimental performance data for absorption refrigeration system using lithium chloride-water solution as the working pair.

Several objectives are formulated to address the overall goal of the present study; these objectives are to:

1- Asses the effect of different variables and operating conditions on the cycle performance, generator temperature, condenser temperature, evaporator temperature and absorber temperature. Also, it is objected to compare the derived thermodynamic data for lithium bromide-water pair with lithium chloride-water pair.

2-Design and install a generator unit as a main part of a single-effect absorption refrigeration cycle using lithium chloride-water solution, to study the effect of regeneration temperature on the rate of water vapour produced inside the generator at constant vacuum pressures and evaluate the minimum generation temperature required to boil off the water from the LiCl-water solution.

3-Study and discuss the effect of inlet solution conditions, (solution temperature and solution flow rate) and generator pressure on the rate of water vapour produced at constant generation temperatures.

2- Theoretical Analysis

Figure (1) shows a block diagram of an absorption refrigeration cycle in the simplest single effect configuration. The cycle consists of an evaporator, condenser, generator, heat exchanger and absorber. High pressure liquid refrigerant coming

from the condenser at state (8) passes into the evaporator through an expansion valve at state (9) that reduces the pressure of the refrigerant to the low pressure existing in the evaporator. The liquid refrigerant (9) vaporizes in the evaporator by absorbing heat from the material being cooled and the resulting low pressure vapor at state (10) passes to the absorber where it is absorbed by the strong solution coming from the generator at state (4) through an expansion valve at state (6), and forms the weak solution at state (1). By weak solution (strong solution) we mean a liquid solution of low (high) absorbent concentration. The weak solution at state (1) is pumped through the solution heat exchanger to extract some energy from the strong solution and then flows into the generator at state (3). In the generator heat is added to the weak solution to boil off some of the refrigerant, the remaining strong solution at state (4) flows back to the absorber and the pure (or nearly pure) refrigerant vapor leaves the generator at state (7) to travel through the condenser at state (8) and thus completes the cycle.

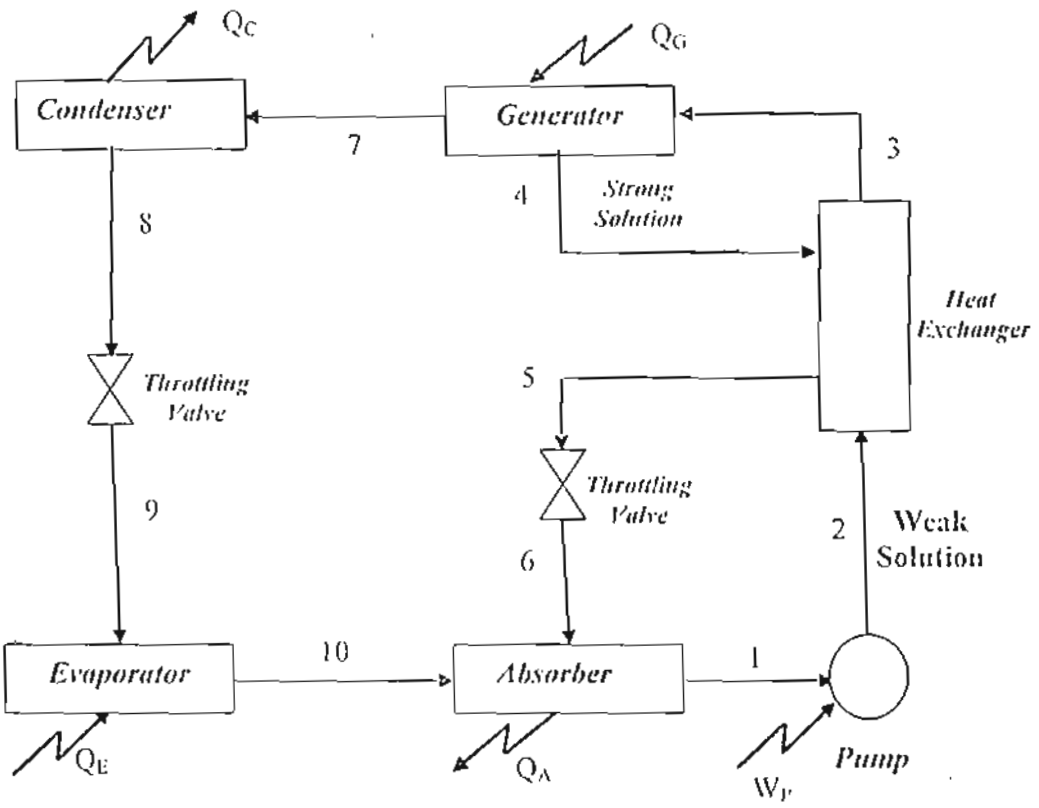

Fig. (1) Block diagram of an absorption refrigeration cycle (single-effect).

Heat and mass balance equations for the system components are presented as follow:

For the refrigerant throttling valve:
The total mass balance:

$$m_8 = m_9 = m_{ref} \quad \text{..... (1)}$$

Where: m_{ref} is the refrigerant mass flow rate, kg/sec

The energy balance;

$$h_8 = h_9 \quad \text{.....(2)}$$

Where: h_8 is the enthalpy of saturated liquid refrigerant at T_8 which equal to condenser temperature T_c, kJ/kg

For the solution throttling valve:

The total mass balance;

$$m_5 = m_6 \quad \text{..... (3)}$$

The energy balance;

$$h_5 = h_6 \quad \text{....(4)}$$

Where: h_5 is the enthalpy of strong solution, kJ/kg.

For the evaporator:

The total mass balance;

$$m_9 = m_{10} = m_{ref} \quad \text{.....(5)}$$

The energy balance;

$$Q_E = m_{ref}(h_{10} - h_9) \quad \text{.....(6)}$$

Where: Q_E is the amount of heat input to the evaporator (cooling capacity); h_{10} is the enthalpy of saturated refrigerant vapor at T_{10}, kJ/kg.

For the generator:

The total mass balance;

$$m_3 = m_7 + m_4 \quad \text{.....(7)}$$

The absorbent mass balance;

$$m_3 x_3 = m_7 x_7 + m_4 x_4 \quad \text{.....(8)}$$

Where: x_3 is the weak solution concentration at state (3), % by weight $kg_{salt}/kg_{solution}$; x_4 is the strong solution concentration at state (4), % by weight $kg_{salt}/kg_{solution}$; x_7 is the absorbent concentration in refrigerant at state (7), (equal zero); m_3 is the weak solution mass flow rate, kg/sec; m_4 is the strong solution mass flow rate, kg/sec and $m_7 = m_{ref}$

The energy balance;

$$Q_G = m_7 h_7 + m_4 h_4 - m_3 h_3 \quad \text{.....(9)}$$

Where: Q_G is the amount of heat added to the generator, kW; h_7 is the enthalpy of refrigerant vapor at T_7, kJ/kg; h_4 is the enthalpy of strong solution at generator temperature T_4 and x_4, kJ/kg and h_3 is the enthalpy of weak solution at T_3 and x_3, kJ/kg

From equations (7) and (8), the strong and weak solution mass flow rate can be evaluated as,

$$m_4 = m_7 \frac{x_3}{x_4 - x_3} \quad \text{..... (10)}$$

$$m_3 = m_7 \frac{x_4}{x_4 - x_3} \quad \text{..... (11)}$$

The flow ratio FR can be defined as the weak solution mass flow rate with reference to the refrigerant mass flow rate as;

$$FR = \frac{m_3}{m_7} = \frac{x_4}{x_4 - x_3} \quad \text{..... (12)}$$

For the absorber:

The total mass balance;

$$m_1 = m_6 + m_{10} \quad \text{..... (13)}$$

The energy balance;

$$Q_A = m_{10} h_{10} + m_6 h_6 - m_1 h_1 \quad \text{.....(14)}$$

Where: Q_A is the amount of heat rejected from the absorber and h_1 is the enthalpy of weak solution at absorber temperature T_1 and x_1, kJ/kg.

For the pump:

The total mass balance;

$$m_1 = m_2 \quad \text{..... (15)}$$

The energy balance:

$$W_p = m_1(h_2 - h_1) \quad \text{..... (16)}$$

Where
W_p is the work consumed by the pump, W.

For the condenser:
The total mass balance;

$$m_7 = m_8 \quad \text{..... (17)}$$

The energy balance;

$$Q_c = m_{ref}(h_7 - h_8) \quad \text{..... (18)}$$

Where: Q_c is the amount of heat rejected from the condenser, W

For the heat exchanger:
The total mass balance;

$$m_2 + m_5 = m_3 + m_6 \quad \text{..... (19)}$$

The energy balance;

$$h_3 = h_2 + \frac{m_4}{m_1}(h_4 - h_5) \quad \text{..... (20)}$$

The heat exchanger effectiveness, k is defined as,

$$k = \frac{m_1}{m_4}\frac{T_3 - T_2}{T_4 - T_2} \quad \text{..... (21)}$$

At steady state, assuming that there are no heat losses, the heat input (to the evaporator and generator) in addition to the work consumed by the pump W_p is equal to the heat rejected (from the absorber and condenser). Hence, the overall heat balance can be represented as,

$$Q_e + Q_G + W_p = Q_A + Q_c \quad \text{.....(22)}$$

The actual coefficient of performance COP of the cycle can be defined as

$$COP = \frac{Q_e}{Q_G + W_p} \quad \text{..... (23)}$$

Neglecting the work consumed by the pump compared to the heat added to the generator Q_G, the cycle coefficient of performance can be calculated as,

$$COP = \frac{Q_e}{Q_G} \quad \text{..... (24)}$$

The pressure of the refrigerant inside the condenser and the evaporator can be calculated according to equation (25) [4] as,

$$LogP = -0.21251 + 3.136119\times10^{-2}T_S - 1.22512\times10^{-4}T_S^2 + 3.6384\times10^{-7}T_S^3 - 5.6707\times10^{-10}T_S^4 \quad \text{.....(25)}$$

Where: P is the pressure of the refrigerant inside the evaporator and condenser, kPa and T_s is the refrigerant saturation temperature, °C.

The enthalpy of the superheated water vapor at outlet from generator can be calculated from [7]. The liquid and vapor enthalpies of the refrigerant can also be calculated from [16].

Thermo physical properties of lithium bromide-water and lithium chloride-water solutions are obtained from lithium bromide chart and reference [11] respectively.

Now, the thermodynamic analysis for the cycle is completed for calculating, the flow ratio and the coefficient of performance within the operational limits for the following range:

For lithium bromide-water cycle:

T_G =55-115°C, T_c =28-46°C, T_k =5-18°C, T_A =24-35°C, weak solution mass flow rate =7 kg/sec, high pressure = 20 kPa and low pressure = 1 kPa.

For lithium chloride-water cycle:
T_G =50-95°C, T_c =28-46°C, T_k =3-18°C, T_A =24-35°C, weak solution mass flow rate =7 kg/sec, high pressure = 20 kPa and low pressure =1 kPa.

Calculation of the Heat Transfer Coefficient

The generation unit is manufactured as a cross flow (single-pass) heat exchanger type, the heat transfer coefficient h_f, W/m^2.K can be evaluated from equation (26) as,

$$h_f = \frac{1}{\left[\frac{1}{u_i} - \frac{1}{h_i} - \frac{1}{h_w}\right]\frac{A_o}{A_i}} \quad \ldots\ldots (26)$$

Where A_o and A_i is the total outlet and inlet area of the copper tubes, m^2; u_i is the overall heat transfer coefficient, $W/m^2.K$; h_i is the hot water heat transfer coefficient, $W/m^2.K$ and h_w is the wall conductance based on inside area, $W/m^2.K$.

The overall heat transfer coefficient u_i can be evaluated from equation (27) as,

$$u_i = \frac{Q_{hw}}{A_i \Delta T_{lm} F} \quad \ldots\ldots (27)$$

Where: Q_{hw} is the hot water heat transfer rate, W and can be evaluated from equation (28) as,

$$Q_{hw} = m_{hw} C_{p\,hw} \left(T_{hw,i} - T_{hw,o}\right) \quad \ldots\ldots (28)$$

Where m_{hw} is the hot water mass flow rate, kg/sec which is a constant value during all experiments and can be measured by weighting a specific volume of hot water which circulate through the generator at a period of time; $C_{p_{hw}}$ is the specific heat of water and can be calculated from [19], kJ/kg.K; $T_{hw,i}$ is the inlet hot water temperature to generator, K; $T_{h.w.o}$ is the outlet hot water temperature from generator, K. $T_{h.w.i}$ and $T_{h\,w,o}$ are measured experimentally.

ΔT_{lm} is the log mean temperature difference, K and can be calculated from equation (29) as,

$$\Delta T_{lm} = \frac{\left(T_{hw,o} - T_i\right) - \left(T_{hw,i} - T_o\right)}{\ln \frac{T_{hw,o} - T_i}{T_{hw,i} - T_o}} \quad \ldots\ldots (29)$$

Where T_i and T_o is inlet and outlet solution temperature, K; F is the correction factor and can be evaluated from [18].

The hot water heat transfer coefficient h_i can be evaluated from equation (30) as,

$$h_i = \frac{Q_{hw}}{A_i \left(T_{hw,av} - T_w\right)} \quad \ldots\ldots (30)$$

Where $T_{hw,av}$ is the average hot water temperature, K and equal to $(T_{hw,i} + T_{hw,o})/2$ and T_w is the wall temperature for the copper tubes, K and measured experimentally by a digital thermometer.

The wall conductance h_w can be evaluated from equation (31) as,

$$h_w = \frac{2\pi K l}{A_i \ln \frac{d_o}{d_i}} \quad \ldots\ldots (31)$$

Where K is the thermal conductivity for the copper tubes, W/m.K and can be evaluated from [19]; d_o and d_i is the outside and inside tube diameter and equal to 0.013 and 0.012 m respectively and l is the tube length 0.32 m.

3- Experimental Set-Up

Figure (2) shows the layout of the experimental set-up, it consists of hot water tank (1) fitted with electrical heater (2). In order to control the temperature of hot water the electrical heater is equipped with a thermostate. A water pump (3) circulates the hot water through the cycle. The lithium chloride-water solution flows from the weak solution tank (6) to regenerate in the generator unit (4). The weak solution tank is fitted with an electrical heater (2) to heat the solution at different temperatures. A vacuum pump (5) is equipped with the generator to remove the water vapor to ambient air and maintained the generator under a certain vacuum pressure. After regeneration the regenerated solution leaves the generator to collect in the strong solution tank. The experimental facilities consist of the following items:

1-Hot water tank, it is used as a reservoir for heating the water at variable temperatures by an electrical heater and manufactured from a galvanized sheet iron 1.5mm thickness; the dimension of the tank is 0.3×0.3×0.5m. The tank is isolated by a thermal isolating material to reduce the heat losses from the tank to the ambient air.

2-Electrical heater, it is used to heat the water and weak solution at variable degrees of temperatures, the heater provides thermal power about 2000W. It is fixed in the bottom of the hot water tank and weak solution tank and connected with electrical thermostat.

3-Hot water pump, It is used to circulate the hot water inside the generator. The type of the pump used in this work is centrifugal type, the power of the pump equals 880W and the speed equals 2850 r.p.m, it gives maximum flow rate 0.029 m^3/min.

4- Generation unit; it is manufactured as a cross flow (single-pass) heat exchanger type as shown in figure (3) and consists of: The outer casing, is manufactured as a rectangular shape from an iron sheet metal 6.00mm thickness, The dimension of the outer casing is 0.44×0.35×0.10m .

The inner shell, is manufactured as a matrix of copper tubes consists of 7 rows and 3 columns which constructed as a staggered array. The tubes having 0.013m outer diameter, 0.012m inner diameter, and 0.5mm thickness, the total length of tubes is 0.34 m and the wetted length is 0.32m, the number of tubes is eighteen and the tubes fixed in the outer casing by welding.

The spray header is manufactured from copper metal with dimension 0.30m length, 0.010m outer diameter and thickness 0.5mm. The number of tubes is three. There are many holes in the top of these tubes to spread the inlet weak solution from the weak solution tank above the inner shell tubes to increase the heat transfer between the weak solution and the hot water.

The sight glasses, they are used to allow flow rate visualization inside the generator. They are manufactured from a fiber material 6.00mm thickness with dimension 0.30×0.15m and the sight glasses fixed at the outer casing by bolts.

5-Vacuum pump, it is used to remove water vapor from the generator and maintained the cycle under a certain vacuum pressures 20, 30 and 40 kPa. The type of vacuum pump used in this work is double stage rotary vane type. The power of the vacuum pump equals 586 W, it gives ultimate vacuum pressure of 0.5 Pa.

6-Weak solution tank [upper tank], it is used as a storage tank from which the weak solution flows to the generator and is manufactured from a galvanized sheet iron 1.5 mm thickness, the dimension of the tank is 0.20×0.20×0.30m. The tank is fitted with an electrical heater (2) to heat the solution at different temperatures.

7- Strong solution tank [lower tank], it is used for collecting the outlet solution from the generator. It has the same shape and dimensions of the weak solution tank.

8- Valves, they are used at several points of the apparatus as shown in figure (2) to control the mass flow rate of the hot water and solution. There are two types of the valves: Ball valves, to control the hot water mass flow rate.

Throttle valves, to control the weak solution mass flow rate and controlling the vacuum pump suction flow rate.

9- Measuring instruments:

Temperature measurements, a digital thermometer is fitted inside the generator to measure the average generation temperature, inlet and outlet temperatures of hot water and strong solution temperature are measured by thermometers (8), (9) and (10) respectively. The weak solution temperature is measured by mercury thermometer. The vacuum pressure inside the generation unit is measured by a pressure gauge (11).

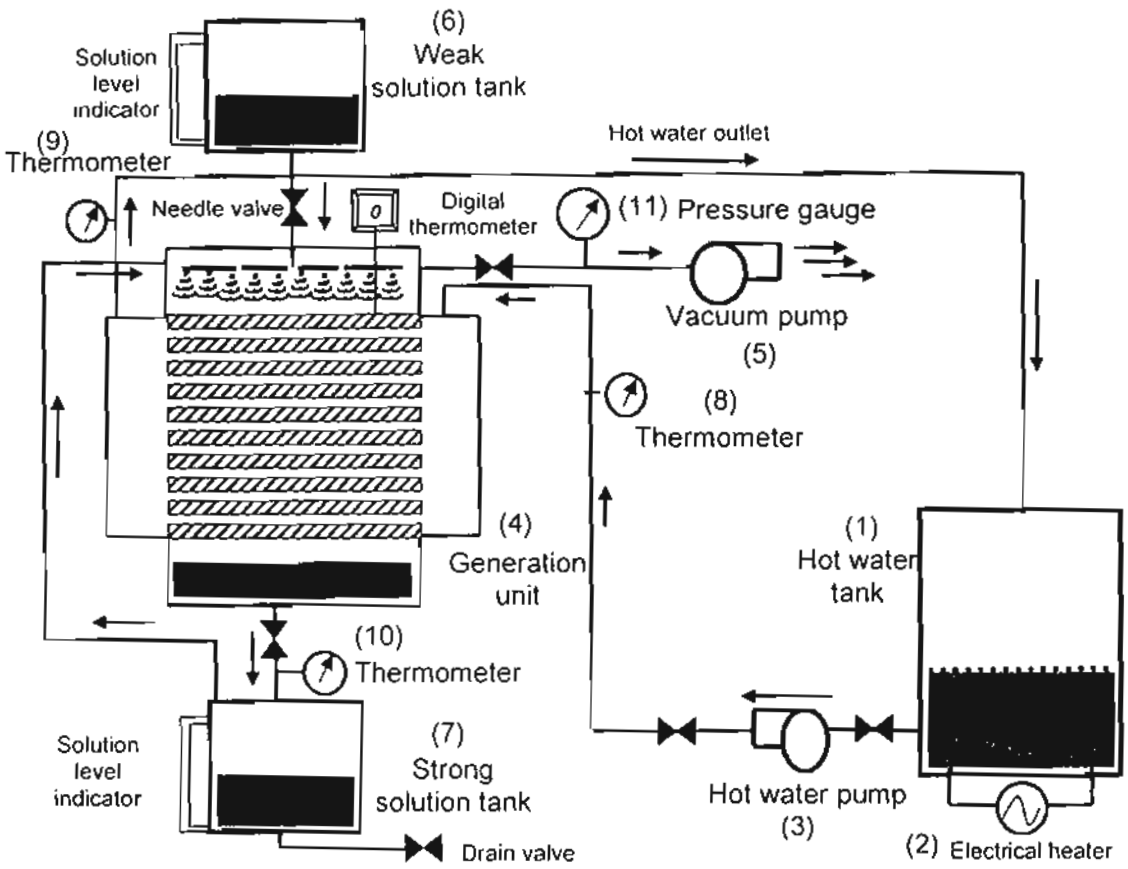

Fig.(2) Schematic of the Experimental Set-Up

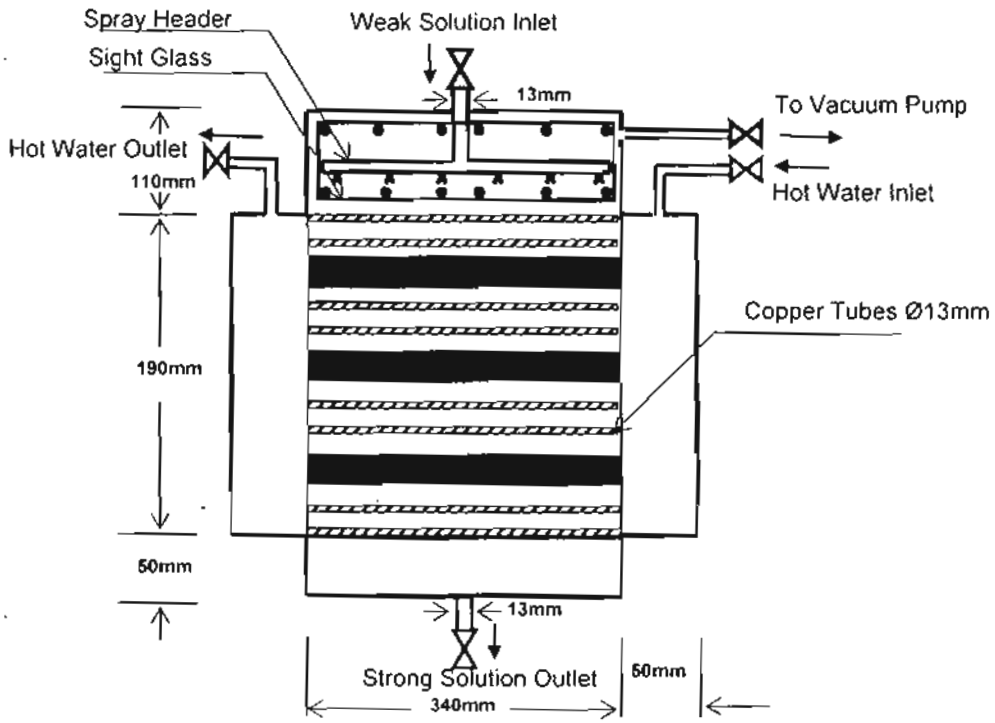

Fig.(3) The Generation Unit

The weak and strong solution concentrations is evaluated by measuring the solution density and temperature. the measured density at a given temperature is then used to find the concentration, which is given as a function of density and temperature in reference [17]. The solution density is evaluated by weighting a sample of solution at inlet and outlet of the generator by a digital balance of 0.02 g resolution and a vessel of 100 cm^3 volumes. The weak solution flow rate is measured by a stop watch and a level indicator connected with weak solution tank.

4- Experimental Procedure

The operation and data collection are carried out as follows. First, the weak solution is put at the weak solution tank at a concentration of 30% and maintained at this value for all runs. switching on the electrical heater and hot water pump, once the required generation temperature and steady state condition is reached the vacuum pump is switched on. At a desired generation pressure, inlet and outlet temperatures of the solution and hot water, average generation temperature and generation pressure are recorded. At the end of the experiment the generated water vapor is calculated. 55 tests are carried out at different inlet solution conditions (temperature and flow rate). generation temperatures and different generation pressure. Then the results are presented graphically.

5- Results and Discussions

5-1 Theoretical Results

5-1-1 Model Validation

A general validation of the model is done by using the derived data obtained from [11] for lithium chloride-water solution. Figure (4) shows the simulated results for the effect of generator temperature on the coefficient of performance at T_E=6°C, T_A=30°C and T_C=40°C. The comparison between results shows a reasonable agreement.

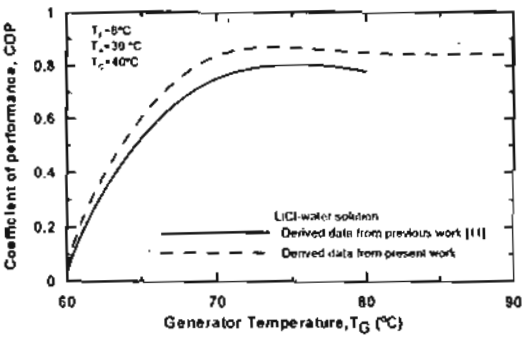

Fig. (4) Comparison between the data obtained from previous work [11] and the present work for the effect of generator temperature on the coefficient of performance for LiCl-water solution

The effect of different operating conditions on the cycle performance and flow ratio for lithium bromide-water cycle are depicted in figures 4, 5, 6 and 7 for the following range of temperatures:

T_G=55-115°C, T_C=29-46°C, T_E=5-18°C, T_A= 24-35°C

Figures (5) and (6) show the variation of the coefficient of performance and flow ratio with the generator temperature at condenser temperature of 29, 36, 42 and 46°C respectively. It can be seen that the coefficient of performance initially increases rapidly until a certain degree of generator temperature, it decreases slightly or become insensitive to any increase in generator temperature. It is also observed that the coefficient of performance is higher at lower condenser temperatures. e.g., at the generator temperature of 90°C, evaporator temperature of 7°C, absorber temperature of 30°C and condenser temperature of 29 and 46°C, the coefficient of performance is 0.869 and 0.836 respectively.

Also it can be seen that the flow ratio decreases as the generator temperature is increased. The rate of decrease in flow ratio is much higher at higher condenser temperatures.

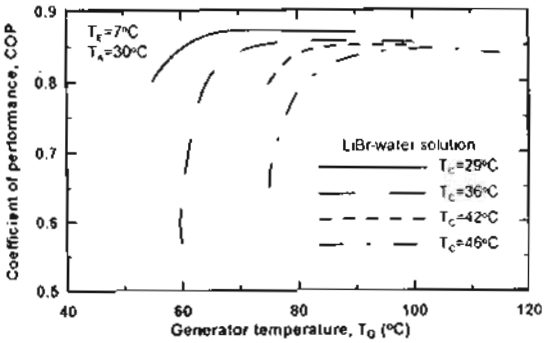

Fig. (5) The effect of generator temperature on the coefficient of performance at different condenser temperatures, T_C

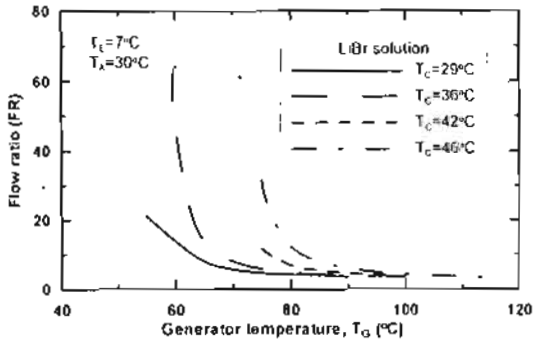

Fig. (6) The effect of generator temperature on the flow ratio at different condenser temperatures, T_C

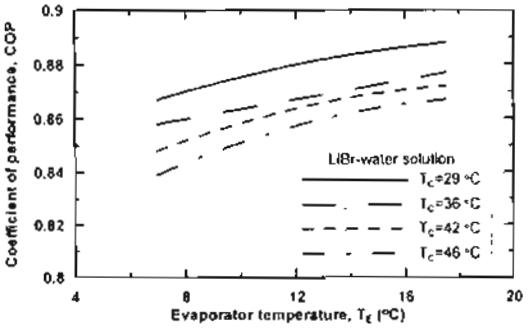

Fig. (7) The effect of evaporator temperature on the coefficient of performance at different condenser temperatures, T_C

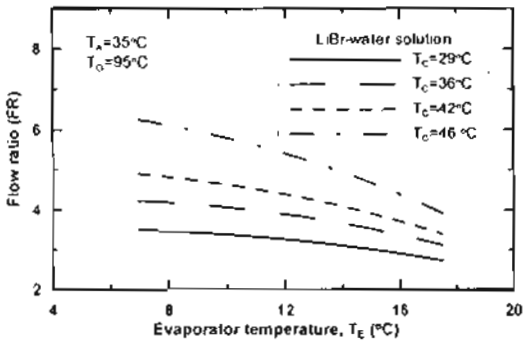

Fig. (8) The effect of evaporator temperature on the flow ratio at different condenser temperatures, T_C

Figures (7) and (8) show the variation of the coefficient of performance and flow ratio with the evaporator temperature at condenser temperatures of 29, 36, 42 and 46°C respectively. It can be seen that the coefficient of performance increases monotonically with an increase in evaporator temperature. It is also observed that the coefficient of performance is higher at lower condenser temperatures. The flow ratio decreases with an increase in evaporator temperature. The rate of decrease in flow ratio is higher at higher condenser temperatures. It is noticed the results in the present work have a good agreement with those obtained by [3].

The effect of different operating conditions on the cycle performance and flow ratio for lithium chloride-water cycle are depicted in figures 9, 10, 11 and 12 for the following range of temperatures:

T_G = 50-95°C, T_E = 29-46°C, T_E = 3-18°C, T_A = 24-35°C.

Figures (9) and (10) show the variation of the coefficient of performance and the flow ratio with the generator temperature at condenser temperatures of 29, 36, 42 and 46°C respectively, from the graphs it can be seen that the coefficient of performance initially increases rapidly but tends to attain a limiting value at higher generator temperatures. It is also observed that the coefficient of performance is higher at lower condenser temperatures. e.g., at the generator temperature of 75°C, evaporator temperature of 7°C, absorber temperature of 30°C and condenser temperature of 29 and 46°C, the coefficient of performance is 0.866 and 0.826 respectively.

The flow ratio decreases as the generator temperature is increased. The rate of decrease in flow ratio is much higher at higher condenser temperatures.

Figures (11) and (12) show the variations of the coefficient of performance and the flow ratio with the evaporator temperature at condenser temperatures of 29, 36, 42 and 46°C respectively.

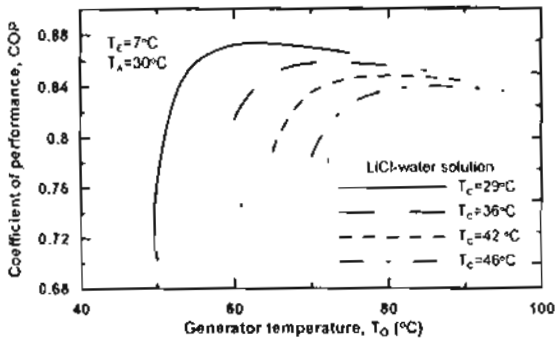

Fig. (9) The effect of generator temperature on the coefficient of performance at different condenser temperatures, T_C

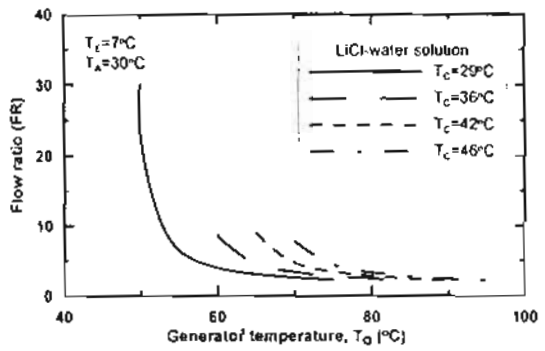

Fig. (10) The effect of generator temperature on the flow ratio at different condenser temperatures, T_C

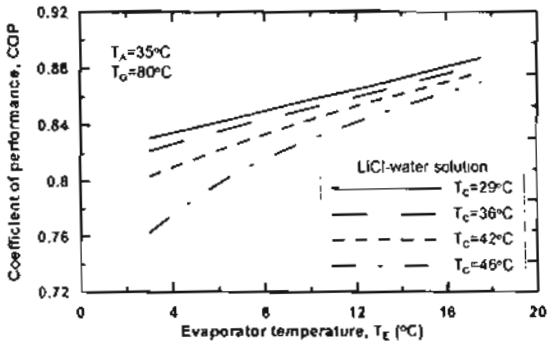

Fig. (11) The effect of evaporator temperature on the coefficient of performance at different condenser temperatures, T_C

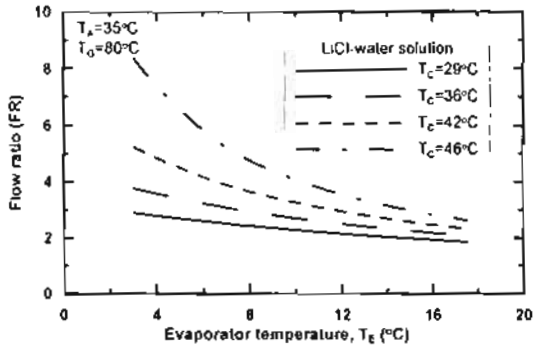

Fig. (12) The effect of evaporator temperature on the flow ratio at different condenser temperatures, T_C

It can be seen that the coefficient of performance increases with an increase in evaporator temperature. It is also observed that the coefficient of performance is higher at lower condenser temperatures. The flow ratio decreases with an increase in evaporator temperature. The rate of decrease in flow ratio is higher at higher condenser temperatures.

comparison between the lithium bromide-water system and lithium chloride-water system.

Figures 13, 14, 15 and 16 illustrate the effect of different operating conditions on the cycle performance and flow ratio for both lithium chloride-water and lithium bromide-water pairs for the following ranges:

T_G=55-95°C, T_E=7-18°C, T_C=29,46°C, T_A = 25, 30°C.

Figures (13) and (14) show the variation of the coefficient of performance and the flow ratio for both the LiCl-water and LiBr-water systems with the generator temperature, at evaporator temperature of 7°C, absorber temperature of 30°C and condenser temperatures of 29 and 46°C respectively. It can be seen that the coefficient of performance for the LiCl-water pair is higher than the LiBr-water case, also the system can operate on the LiCl-water pair at much lower flow ratios than that for the LiBr-water pair.

Figures (15) and (16) show the variation of the coefficient of performance and the flow ratio with the evaporator temperature at condenser temperature of 46°C, generator temperature of 80°C and absorber temperature of 25 and 30°C respectively. It can be seen that the coefficient of performance increases while the flow ratio decreases with an increase in evaporator temperature.

Based on this comparison it may appear that the system can operate on the LiCl-water pair at much lower flow ratios than that for LiBr-water pair, and the COP is higher for the LiCl-water pair. So,

lithium chloride is a better choice of absorbent.

However other physical properties like viscosity should also be considered. Aqueous solutions of lithium chloride have higher viscosities than lithium bromide solutions. Thus absorption systems operating with lithium chloride solutions will have a higher load on the solution circulation pump.

Finally, the importance of derived thermodynamic data as flow ratio is that the flow ratio determines the size of the various items of equipment. an increase in the flow ratio affects the performance in the following ways [11]:

- The concentration difference between the absorber and generator decreases.
- The heat losses from the system become higher.
- The power required for the solution pump increases.

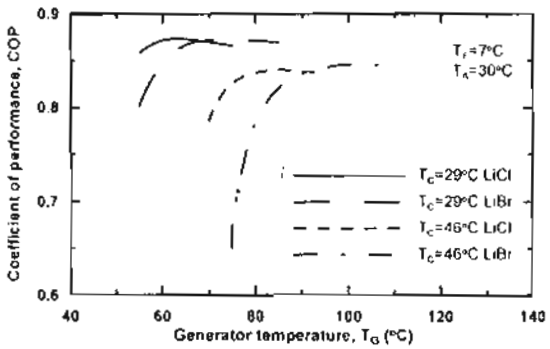

Fig. (13) The effect of generator temperature on the coefficient of performance at different condenser temperatures, T_C for LiCl and LiBr systems

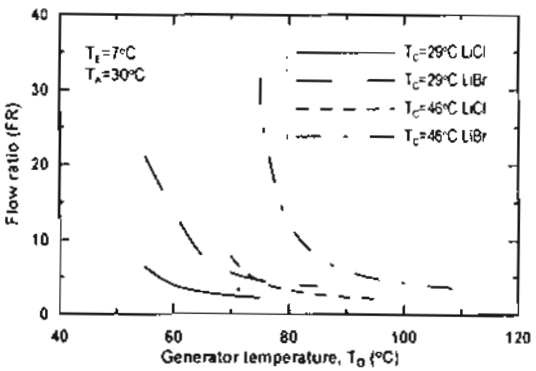

Fig. (14) The effect of generator temperature on the flow ratio at different condenser temperatures, T_C for LiCl and LiBr systems

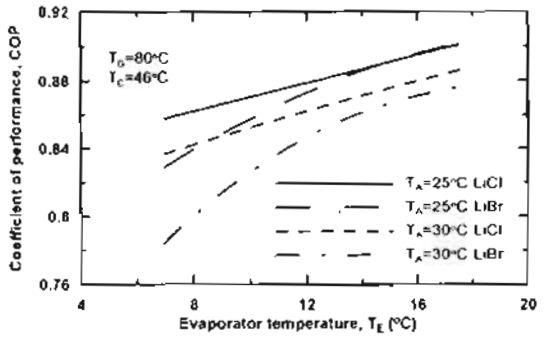

Fig. (15) The effect of evaporator temperature on the coefficient of performance at different absorber temperatures, T_A for LiCl and LiBr systems.

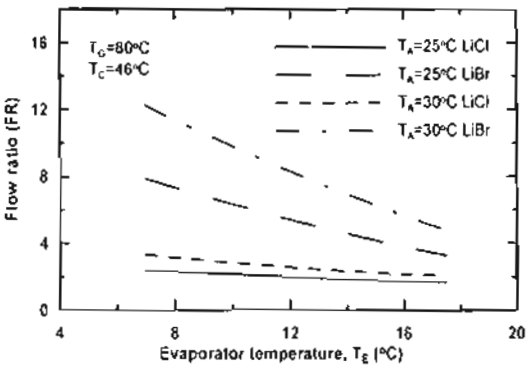

Fig. (16) The effect of evaporator temperature on the flow ratio at different absorber temperatures, T_A for LiCl and LiBr systems

5-2 Experimental Results

A total of 55 data runs are taken under various operating conditions. The input variables used in the experiments are, generator temperature, inlet solution temperature, and generator pressure. For all experiments, the inlet solution concentration and the inlet solution mass flow rate are fixed at a value of 30% and 0.0024kg/sec respectively. The output parameters is measured or calculated from experimental data. The measured output parameters are outlet solution concentration and temperature, the calculated output parameters are, mass of generated vapour, flow ratio, amount of heat added, overall film heat transfer coefficient and coefficient of performance. The range of operating conditions employed in this research is presented in table (1).

Table (1) Range of operating conditions:

Inlet solution temperature (°C)	22 : 60
Inlet solution concentration (%)	30
Inlet solution mass flow rate (kg/sec)	0.0024
Generator temperature (°C)	59 : 90
Generator pressure (kPa)	20 : 40
Number of tests	55

Figures (17) and (18) show the variation of the rate of water vapor produced with the generator temperature for different runs, at generator pressure of 20, 30 and 40kPa, inlet solution mass flow rate of 0.0024kg/sec, inlet solution temperature at the range (22:59.6°C) and inlet solution concentration of 30% respectively. It can be noted that the mass of water vapor generated inside the generator is increased with an increase in generator temperature. For the same conditions (generator temperature, inlet solution temperature and inlet solution mass flow rate) the rate of water vapor is higher at lower generator pressure, e.g., at generator temperature of 76°C, inlet solution temperature of 22°C, inlet solution mass flow rate of 0.0024 kg/sec and generator pressure of 20, 30 and 40 kPa, the rate of water vapor is 0.108, 0.072 and 0.061 kg/hr respectively

An increase in inlet solution temperature and for the same conditions results in increase the rate of water vapor generated, e.g., at generator temperature of 76°C, generator pressure of 20 kPa , inlet solution mass flow rate of 0.0024 kg/sec and inlet solution temperature of 22 and 59.6°C, the rate of water vapor is 0.108 and 0.244 kg/hr respectively.

Also from figures, it can be observed that for generator pressure equal 40 kPa there is a minimum generator temperature which can be used to boil off the water from the solution approximately (65°C).

The most important parameters are deceasing the generator pressure and increasing the inlet solution temperature, this results show the important of using a heat exchanger in any absorption refrigeration cycle.

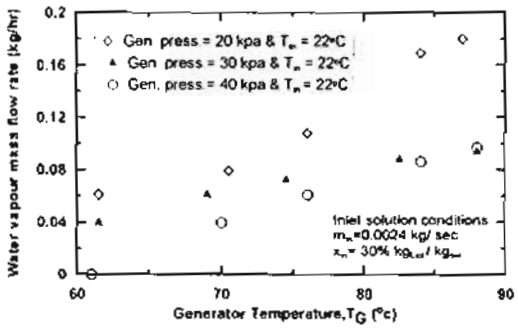

Fig (17) The effect of generator temperature on the water vapour mass flow rate at different generation pressures and inlet solution temperatures

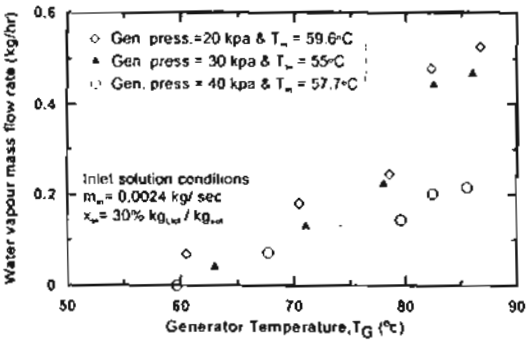

Fig (18) The effect of generator temperature on the water vapour mass flow rate at different generation pressures and inlet solution temperatures

Figures (19) and (20) show the variation of the flow ratio with the generator temperature for different runs. It can be seen that the flow ratio decreases as the generator temperature is increased. For the same conditions, an increase in inlet solution temperature decrease the value of the flow ratio, e.g., at generator temperature of 87°C, inlet solution mass flow rate of 0.0024 kg/sec, generator pressure of 20 kpa and inlet solution temperature of 22 and 59.6°C the flow ratio is 49.1 and 16.8 respectively. It is also observed that the rate of decrease in flow ratio is much higher at higher generation pressure.

Figures (21) and (22) show the effect of generator temperature on the outlet

solution temperature from the generator (strong solution) for different runs, as expected, the outlet solution temperature increases as the generator temperature is increased. It can be noted that for the same conditions an increase in generator pressure results in increase in the outlet solution temperature, e.g., at generator temperature of 76°C, inlet solution temperature of 22°C, inlet solution mass flow rate of 0.0024 kg/sec and generator pressure of 20, 30 and 40 kPa, the outlet solution temperature is 64, 63 and 62°C respectively.

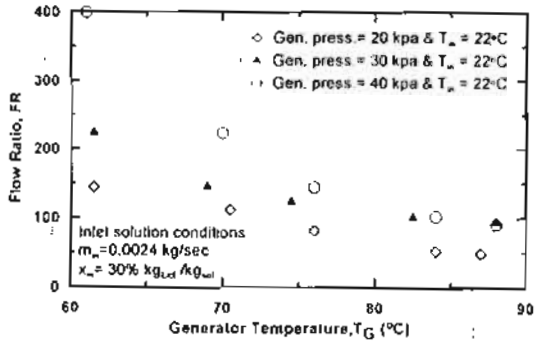

Fig (19) The effect of generator temperature on the flow ratio at different generation pressures and inlet solution temperatures

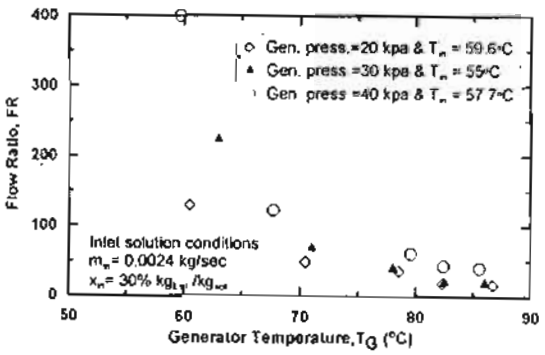

Fig (20) The effect o f generator temperature on the flow ratio at different generation pressures and inlet solution temperatures

Figures (23) and (24) show typically the experimental results of the outlet solution concentration (strong solution) with generator temperature for different runs. It can be observed from these figures that the outlet solution concentration increases with an increase in the generator temperature. As is shown, at the conditions where generator pressure equal 40 kPa a minimum generator temperature must be used (approximately 65°C) to boil off the water from the (LiCl-water) solution, then getting a variation in outlet solution concentration. Finally the outlet solution concentration is higher for higher generation temperature (up to 80°C).

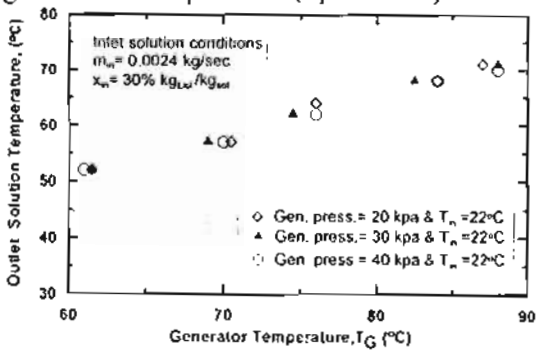

Fig (21) The effect of generator temperature on the outlet solution temperature at different generation pressures and inlet solution temperatures

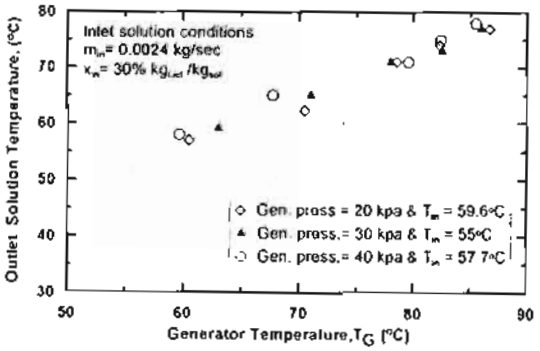

Fig (22) The effect of generator temperature on the outlet solution temperature at different generation pressures and inlet solution temperatures

Also it can be noted that for the same conditions, an increase in the inlet solution temperature increases the outlet solution concentration. e.g., at generator temperature of 82.5°C, generator pressure of 30 kPa, inlet solution mass flow rate of 0.0024 kg/sec and inlet solution temperature of 22 and 55°C, the outlet solution concentration is 30.3 and 31.57 respectively.

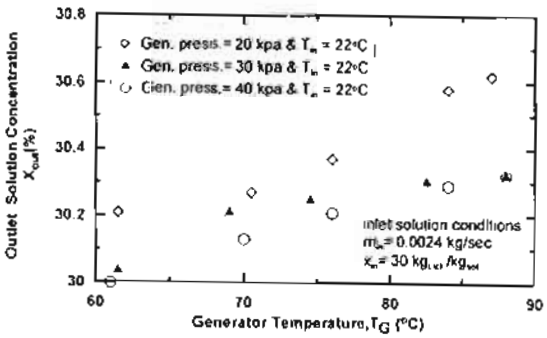

Fig (23) The effect of generator temperature on the outlet solution concentration at different generation pressures and inlet solution temperatures

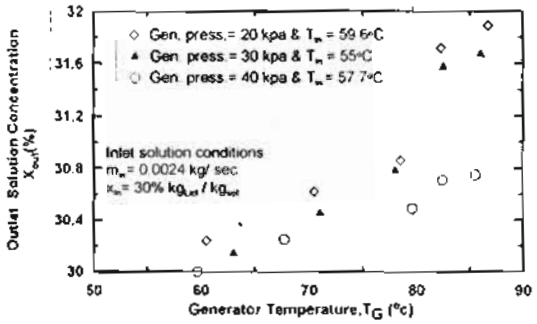

Fig (24) The effect of generator temperature on the outlet solution concentration at different generation pressures and inlet solution temperatures

Figures (25) and (26) show the relation between the generator temperature and the amount of heat added to the generator, Q_G for different runs. As expected the results show that the amount of heat added to generator increases with an increase in generator temperature. Also it can be observed that an increase in inlet solution temperature and a decrease in generation pressure results in increase the total heat added to generator.

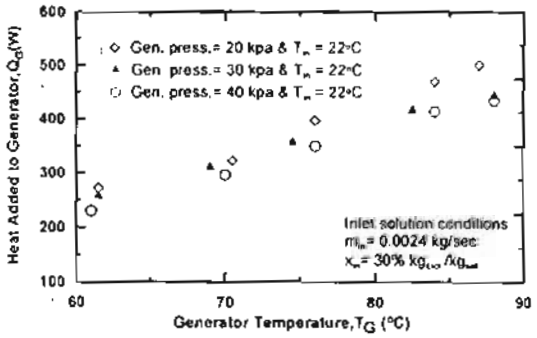

Fig (25) The effect of generator temperature on the amount of heat added to generator at different generation pressures and inlet solution temperatures

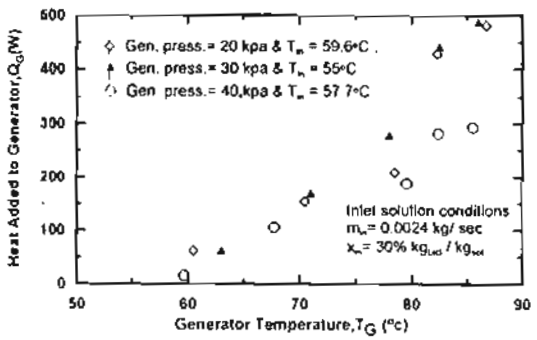

Fig (26) The effect of generator temperature on the amount of heat added to generator at different generation pressures and inlet solution temperatures

Figures (27) and (28) show the relation between the generator temperature and the heat transfer coefficient h_f. It can be indicated that the trend of heat transfer coefficient is varied random with an increase in generator temperature, this because there are many factors affected in calculations of heat transfer coefficient as explained in the theoretical analysis.

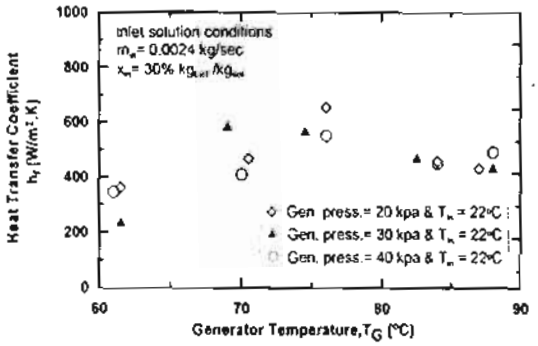

Fig (27) The effect of generatortemperature on the film heat transfer coefficient at different generation pressures and inlet solution temperatures

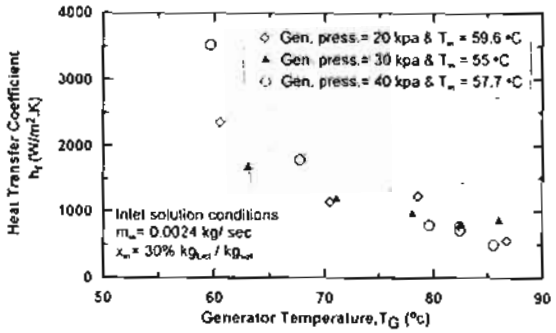

Fig (28) The effect of generator temperature on the film heat transfer coefficient at different generation pressures and inlet solution temperatures

Figures (29) and (30) show the effect of generator temperature on the coefficient of performance of the absorption refrigeration cycle for different runs. It can be observed that the coefficient of performance, COP increases with an increase in generator temperature until a certain generator temperature approximately (79:83°C) for all runs then the COP decreases slightly or become insensitive to any increase in the generator temperature.

Also it can be noted that, at the same conditions the COP is higher at lower generator pressure, e.g., at the generator temperature of 76°C, inlet solution temperature of 22°C, inlet solution mass flow rate of 0.0024 kg/sec and generator pressure of 20, 30 and 40 kPa, the coefficient of performance is 0.187, 0.147 and 0.120 respectively.

Also, the COP is higher at higher inlet solution temperature.

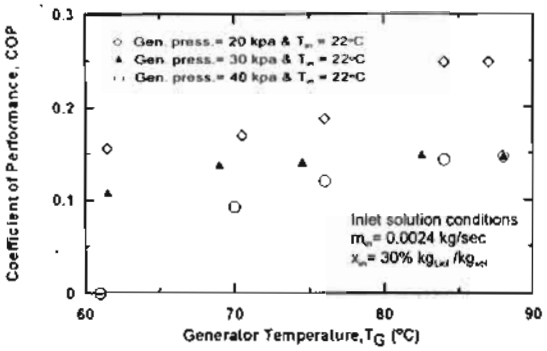

Fig (29) The effect of generator temperature on the coefficient of performance, COP at different generation pressures and inlet solution temperatures

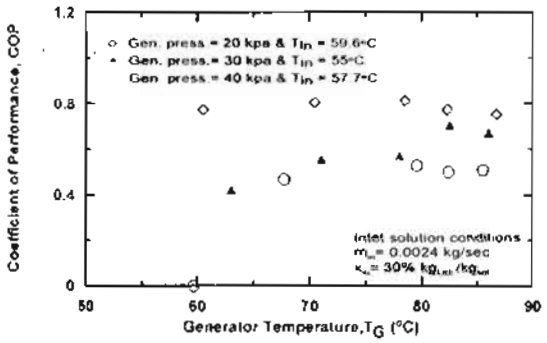

Fig (30) The effect of generator temperature on the coefficient of performance, COP at different generation pressures and inlet solution temperatures

6- Conclusions

A theoretical model describing the effect of different operating temperatures on the flow ratio and the coefficient of performance is presented for the absorption cycle using the LiCl-water pair and the LiBr-water pair. The thermodynamic analysis of the two cycles show that the COP increases with an increase in generation temperature until a certain value of generator temperature, then it decreases slightly or become insensitive to any increase in generator temperature. An increase in evaporator temperature, or decrease in the condenser and the absorber temperatures increases the COP.

The data obtained for the LiCl-water system are compared with that obtained for the LiBr-water system.

A generation unit in an absorption refrigeration cycle uses a lithium chloride-water solution as the working pair has been constructed and experimentally studied to evaluate the effect of different operating conditions on the rate of water vapor produced inside the generator and the cycle coefficient of performance.

The results are plotted and have revealed these findings:

1-The COP is higher for the LiCl-water pair than that for LiBr-water pair. for identical conditions.

2-The flow ratio FR is lower for the LiCl-water pair when compared with that for LiBr-water pair.

3-The LiCl-water pair can be used for a lower range of generator temperatures and hence is suitable for solar absorption refrigeration systems. e.g., at different operating conditions, the maximum COP is obtained at generator temperature at the range (65-85°C).

4-For specific design parameters, a suitable generation temperature must be chosen in order to boil off the water from the LiCl-water solution. e.g., at generation pressure of 40 kPa a minimum generation temperature required is 65°C

5-Inlet solution temperature and generation pressure have a significant effect on the water vapor generation rate.

6-The maximum coefficient of performance obtained from measured data is 0.812.

Nomenclature

A_i	Total inside area of copper tubes, m^2.
A_o	Total outside area of copper tubes, m^2.
COP	Coefficient of performance.
C_p	Specific heat, kJ/kg.K.
d	Diameter of copper tube, m.
F	Correction factor.
FR	Flow ratio.
h	Enthalpy of solution or refrigerant, kJ/kg.
h_f	Film heat transfer coefficient, $W/m^2.K$.

h_i	Heat transfer coefficient based on hot water side, $W/m^2.K$.
h_w	Wall heat transfer coefficient, $W/m^2.K$
l	Tube length, m.
k	Heat exchanger effectiveness.
K	Thermal conductivity.
m	Mass flow rate, kg/sec.
m_{in}	Inlet solution mass flow rate, kg/sec.
P	Pressure, kPa.
Q	Heat transfer rate, W.
T	Temperature, °C or K.
u_i	Overall heat transfer coefficient, $W/m^2.K$.
W_p	The work consumed by the pump, W.
x	Solution concentration, %.

Greek symbols

Δ	Difference

Subscripts

A	Absorber
C	Condenser
E	Evaporator
G	Generator
gen	Generation
h.w	Hot water
h.w,av	Average hot water
h.w,i	Inlet hot water
h.w,o	Outlet hot water
i or in	Inlet
L	Liquid
o	Outlet
p	Pump
ref	Refrigerant
s	Saturation
sol	Solution
V	Vapor
W	Wall

Reference

1-W. Saman, M. Krause, K. Vajen, "Solar Cooling Technologies Current Status and recent Developments," Sustainable Energy Centre, University of South Australia, the Mawson Lakes Compus, Mawson Lakes, SA 5095, 2004.

2-Alaktiwi, M. Mostafavi and B. Agnew, "Experimental and Optimization Studies on the Operating Characteristics of a Water-Lithium Bromide Absorption Refrigeration System," 3rd Jordanian Mechanical & Industrial Engineering Conference, 1999.

3-Gershon Grossman, "Solar Powered Systems for Cooling, Dehumidification and Air-Conditioning," Solar Energy," Vol.72, No.1, PP. 53-62, 2002 **4-Arzu Sencan, Kemal A. Yakut, Soteris A. Kalagiron,** "Thermodynamic Analysis of Absorption Systems Using Artificial Neural Network," Renewable Energy PP. 1-15,2005

5-ASHRAE, "Handbook of Fundamentals, "Atlanta, Gad, PP. 14.1-14.8, 1983.

6-Grossmon G. and Johannsen A., "Solar Cooling and Air-Conditioning," Progress in Energy and Combustion, Science 7, PP.185-228, 1981.

7-Harries, A. W. and C. N. Chen, "Operational Dynamics of Coupled Plate Solar Collector and Absorption Cycle Heat Pump system with Energy Storage," Appeared in Heat Transfer in Solar Energy System, published by ASME, PP.103-111, 1977.

8-K. Sumathy, Z. C. Huang and Z. F. Li, "Solar Absorption Cooling with Low Grade Heat Source a Strategy of Development in South China," Solar Energy, Vol. 72, No.2, PP. 155-162, 2002.

9-Gommed k. and Grossman G., "Performance Analysis of Staged Absorption heat Pumps, Water-Lithium Bromide Systems," ASHRAE Transactions 1996 (part 1), 1590-1598.

10-WWW. Newbuildings. Org. "Absorption Chillers" Soutbern California Gas Company, Newbuildings Institute, Advanced Design Guide Line Series 1998.

11-G. S. Grover, S. Devotta and F. A. Holland, "Thermodynamic Design Data for Absorption Heat Pump Systems Operating on Water-Lithium Chloride: part one, Cooling," Heat Recovery Systems & CHP Vol. 8, No. 1, PP.33-41, 1988.

12-G. S. Grover, S. Devotta and F. A. Holland, "Thermodynamic Design Data for Absorption Heat Pump Systems Operating on Water-Lithium Chloride: part two, Heating," Heat Recovery Systems & CHP Vol. 8, No.5, PP.419-423, 1988.

13-S. K. Chaudhari, D. V. Paranjape, M. A. R. Eisa and F. A. Holland, "A Comparative Study of the Operating Characteristics of Water-Lithium Chloride and Water-Calcium Chloride Absorption Heat Pumps," Heat Recovery Systems, Vol. 6, No. 1, PP. 39-46, 1989.

14-S. K. Chaudhari, and K. R. Patil, "Thermodynamic Properties of Aqueous Solution of Lithium Chloride," Physics and Chemistry of Liquids, Vol. 40, No. 3, PP. 317-325, 2002.

15-S. H. Won and W. Y. lee, "Thermodynamic Design Data for Double-Effect Absorption Heat Pump Systems using Water-Lithium Chloride-Cooling." Heat Recovery Systems & CHP Vol. 11, No. 1, PP. 41-48, 1991.

16-Elsayed, M. M., I. S. Taha and J. A. Sabbagh, "Design of Solar Thermal Systems," King Abdulaziz University, Faculty of Engineering, 1986.

17-Zaetsev ED, Assev GG., "Physical Chemical Properties of Binary Non-Organic Solutions." Khemia ; 1988, [in Russian].

18-R. A. Bowman, A. C. Mueller, and W. M. Nagle, "Mean temperature difference in design, Trans." ASME, Vol. 62, 1940, pp. 417-422.

19-Adrian Began, "Heat Transfer," 1993.